Polymer Journal (2017) 49, 671–676

www.nature.com/pj

ORIGINAL ARTICLE

Sulfonated polyimide/ionic liquid composite membranes for carbon dioxide separation

Akika Ito[1,3], Tomohiro Yasuda[2,3], Xiaofeng Ma[1] and Masayoshi Watanabe[1]

A series of composite membranes (SPI-NTf$_2$ and SPI-PF$_6$) consisting of a sulfonated polyimide (SPI) and an ionic liquid (IL), either [C$_4$mim][NTf$_2$] or [C$_4$mim]PF$_6$, where [C$_4$mim] and [NTf$_2$] stand for 1-butyl-3-methylimidazolium and bis(trifluoromethanesulfonyl)amide, respectively, were prepared, and their thermal, mechanical and gas (carbon dioxide (CO_2) and N_2) permeation properties were systematically investigated. The ILs functioned as plasticizers of the SPI, making the composite membranes softer (lower Young's modulus and larger elongation at break). However, SPI-NTf$_2$ (75), containing 75 wt % [C$_4$mim][NTf$_2$], still exhibited a Young's modulus higher than 10 MPa, which is much higher than that reported for common IL/polymer composites. The SPI membrane behaved as a gas barrier membrane; however, the addition of IL greatly enhanced gas permeability. Consequently, SPI-NTf$_2$ (75) exhibited CO_2 permeability (P_{CO_2}) of 412 Barrer at 30 °C and selectivity against N_2 (P_{CO_2}/P_{N_2}) of 27. The SPI-PF$_6$ composite membranes showed similar behavior; however, gas permeability exhibited by these membranes was lower than that exhibited by the SPI-NTf$_2$ composite membranes. In permeation tests under mixed-gas conditions, the P_{CO_2} value decreased than that under single-gas conditions, whereas P_{N_2} increased, and P_{CO_2}/P_{N_2} decreased (from the range 29 – 27 to 12–16).
Polymer Journal (2017) **49,** 671–676; doi:10.1038/pj.2017.31; published online 21 June 2017

INTRODUCTION

The reduction of carbon dioxide (CO_2) emissions resulting from combustion of fossil fuels is recognized as a crucial issue because of its significant impact on global climate change and other associated problems.[1,2] Therefore, CO_2 capture and separation is becoming a serious concern and of great importance for mitigating such environmental issues. Hydrogen (H_2) purification,[3] natural gas treatment[4] and the removal of CO_2 from gas streams are related technologies for efficient fossil fuel utilization.[5] Up to now, four methods have been proposed and used in CO_2 capture and separation: absorption in a liquid phase,[6–8] adsorption on highly porous materials,[9,10] membrane separation[6] and cryogenic condensation.[11] Among them, membrane separation technology requires smaller operational energy and lower running costs as compared with the other more energy consumptive methods, especially in small- and medium-scale separations.[12,13]

For membrane separation of CO_2, supported ionic liquid membranes (SILMs),[14–17] polymeric membranes[18–22] and ion-gel membranes[23–27] have been developed. SILMs are polymeric or inorganic porous materials filled with ionic liquids (ILs). They exhibit higher permeability and selectivity of CO_2 than other polymeric membranes, which generally exhibit limited CO_2 diffusion in their rigid polymer matrix. These SILMs are favorable for gas separation because of their high CO_2 selectivity, which is owing to the higher solubility of CO_2 in IL than other gases, such as O_2, H_2, N_2 and CH_4.[14–17,28] The unique properties of ILs, such as their negligible vapor pressure, high thermal and chemical stability, and low flammability,[29–31] also contribute to the stability and durability of SILMs. However, SILMs cannot hold ILs under pressurized conditions because ILs in the pores are physically held by weak capillary forces, which is a serious problem for gas separation membranes.[17] Ion gels, which are polymeric networks swollen by an IL or by IL mixtures,[32] have recently been developed as promising materials for CO_2 separation membranes to solve the problem of SILMs.

Generally, polymer gels are classified into two categories, that is, chemical gels and physical gels. The same classification can also be made for ion gels. Chemical ion gels are formed by covalent crosslinking of IL-compatible polymers. For example, we developed a series of chemical ion gels by *in situ* polymerization of vinyl monomers in ILs.[33] Physical ion gels are typically formed by microphase-separated structures of amphiphilic block copolymers,[34–40] in which IL-incompatible segments[41,42] aggregate and serve as the physical crosslinking points. Both classes of ion gels have been applied to CO_2 separation membranes and both exhibit favorable separation properties without any leakage issues. However, because of their lower mechanical properties, both classes of ion-gel membranes need to be relatively thick (>1 mm) to maintain

[1]Department of Chemistry and Biotechnology, Yokohama National University, Yokohama, Japan and [2]Research and Development Division, Institute for Catalysis, Hokkaido University, Sapporo, Japan
[3]These authors contributed equally to this work.
Correspondence: Professor M Watanabe, Department of Chemistry and Biotechnology, Yokohama National University, 79-5 Tokiwadai, Hodogaya-ku, Yokohama 240-8501, Japan.
E-mail: mwatanab@ynu.ac.jp
Received 24 February 2017; revised 10 May 2017; accepted 18 May 2017; published online 21 June 2017

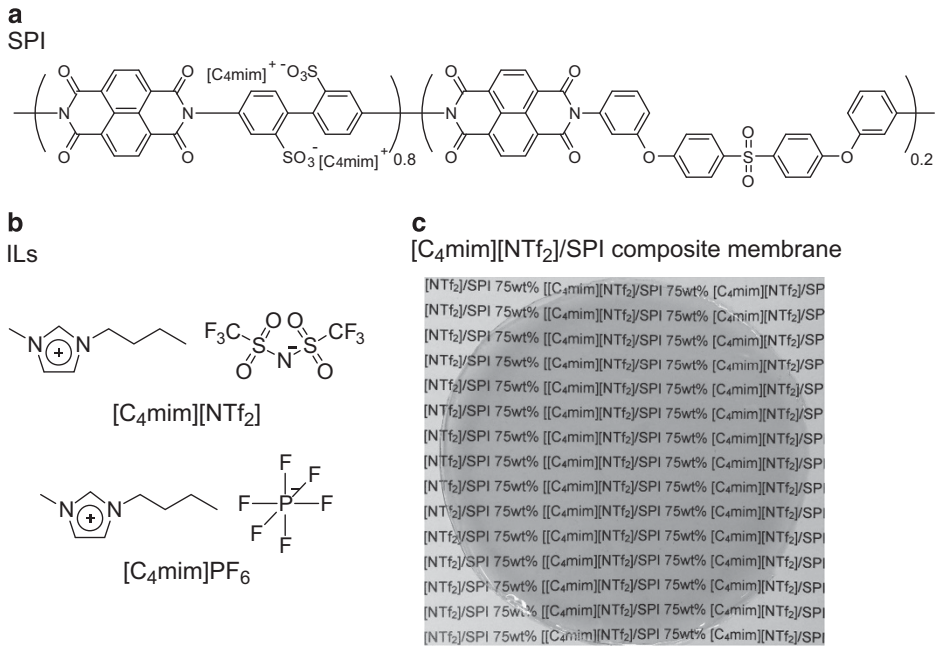

Figure 1 Chemical structures of (**a**) sulfonated polyimide (SPI), (**b**) ionic liquid (ILs) ([C_4mim][NTf_2] and [C_4mim][PF_6]) and (**c**) a photograph of [C_4mim][NTf_2] composite membrane. A full color version of this figure is available at the *Polymer Journal* journal online.

membrane integrity. This thickness leads to lower permeability because the permeability of separation membranes depends on the ratio of the permeability coefficient to the membrane thickness.[43] We, therefore, were interested in developing mechanically reliable CO_2 separation membranes.

Up to now, we reported a series of thin and tough composite membranes ($<100\,\mu m$) consisting of an IL and a sulfonated polyimide (SPI) having a cation in common with the IL.[44,45] These membranes consist of excellent mechanical properties, which have never been achieved for conventional ion-gel membranes, in addition to good thermal stability and high ionic conductivity.[46] These composite membranes have been applied to non-humidified intermediate temperature fuel cells[47] and actuators.[48] Thus, we considered that these composite membranes can also be possible candidate as CO_2 separation membranes.

In this work, we prepared IL/SPI composite membranes comprising a hydrophobic IL, either [C_4mim][NTf_2] or [C_4mim]PF_6, and an SPI containing [C_4mim] as a counter cation. Membranes were fabricated using the solution casting method. These membranes were characterized via their thermal and mechanical property measurements. Furthermore, CO_2 separation performance of the membranes was explored.

EXPERIMENTAL PROCEDURES

Materials

1-Bromobutane (98%) and triethylamine (99%; Wako Chemicals, Takasaki, Japan) was used as received. 1-Methylimidazole (99%; Tokyo Chemical Industry, Tokyo, Japan) was distilled under vacuum before use. Lithium bis(trifluoromethanesulfonyl)amide (Morita Chemicals, Osaka, Japan) and sodium hexafluorophosphate (97%; Wako Chemicals) were stored in Ar atmosphere grove box. Bis[4-(3-aminophenoxy)-phenyl]sulfone (98%; Tokyo Chemical Industry) was recrystallized from ethanol/water solution. 1,4,5,8-Naphthalene-tetracarboxylicdianhydride (Sigma-Aldrich, St Louis, MO, USA) was poured into *N*,*N*-dimethylformamide and resulting suspension was stirred at 60 °C for a day to remove soluble impurity. Pure 1,4,5,8-naphthalene-tetracarboxylicdianhydride was corrected by filtration, washed with acetone several times and dried under vacuum. 2,2′-Benzidinedisulfonic acid (70%; Tokyo Chemical Industry) was purified as follows: purchased 2,2′-benzidine-disulfonic acid was dissolved in deionized water including excess amount of triethylamine and the solutions was filtered. Addition of 1 M HSO_4 aqueous solution to the solution afforded precipitation of pure 2,2′-benzidinedisulfonic acid as white powder. The white power was washed with water several times and dried under vacuum.

Membrane preparation

[C_4mim][NTf_2] and [C_4mim]PF_6 were synthesized and purified according to a previously reported method,[49] and their structure was identified by ^{1}H NMR. SPI was also synthesized by a previously reported method,[46] and its counter cation was exchanged with [C_4mim] by immersing it in a methanol solution of [C_4mim][NTf_2].[48] Composite membranes were prepared by the solution casting method according to a previously reported method.[46] The chemical structures of [C_4mim][NTf_2], [C_4mim]PF_6 and the SPI in [C_4mim] form and the appearance of the composite membranes are shown in Figure 1.

Thermal analyses

Differential scanning calorimetry (DSC) measurements were carried out using a Hitachi High-Tech DSC 6220 (Hitachi High-Technologies, Tokyo, Japan) under a N_2 atmosphere. The samples were tightly sealed in aluminum pans in a glove box ([H_2O] < 1 p.p.m.). The measuring pans in the DSC apparatus were heated to 150 °C, cooled to −150 °C and then heated again to 150 °C. The cooling and heating rates were 10 °C min^{-1}. The DSC curves were recorded during the reheating scans. Thermogravimetric analysis of the composite membranes was carried out using a Seiko Instruments TG-DTA 6200C (Seiko Instruments, Chiba, Japan) under a N_2 atmosphere. The samples were weighed and placed in aluminum pans. Then, they were heated to 100 °C and maintained at that temperature for 30 min under N_2 atmosphere to remove included water. After cooling to room temperature, they were heated again to 550 °C at a heating rate of 10 °C min^{-1} and the thermogravimetric curves were recorded.

Tensile tests

Tensile tests were performed with a Shimadzu EZ-LX 10N (Shimadzu, Kyoto, Japan) under an ambient atmosphere. Samples were cut into dumbbell shapes (JIS K6251, 35×6 mm^2 (total) and 12×2 mm^2 (test area)) using a Kobunshi-

Keiki dumbbell cutter (Koubunshi Keiki, Kyoto, Japan). Stress–strain curves were measured by stretching the samples at a head speed of 1 mm s^{-1}.

Gas permeability measurement

CO_2 and N_2 permeability was measured with a gas permeation measurement apparatus, GTR-10XFKS (GTR-Tech, Kyoto, Japan), and the concentration of the permeated gases was quantified using a gas chromatograph, Yanaco G2700T (Yanaco Technical Science, Tokyo, Japan), with a thermal conductivity detector. Helium was used as the carrier gas for the measurement of CO_2 and N_2 concentrations. The membranes were placed at the center of the permeation cell (permeation area was 9.62 cm^2), and the test gas (either CO_2 or N_2/mixed CO_2 and N_2 (2:1 by volume)) was introduced to one side of the membrane at a flow rate of 30 ml min^{-1}. The carrier gas was introduced to the other side of the membrane at a flow rate of 50 ml min^{-1}, and the concentration of the permeated gas was analyzed by the gas chromatograph. A pressure of carrier gas and a total pressure of test gas were set at 76 cm Hg (atmospheric pressure), respectively. The measurements were conducted five times for a single membrane to estimate gas permeability, and the average was adopted as the result. The gas permeability coefficients, P_{CO_2} and P_{N_2} (Barrer $= 1 \times 10^{-10}$ cm^3 (STP) cm cm^{-2} s^{-1} cm Hg^{-1}), were calculated using the following equation:

$$P(\text{Barrer}) = \frac{Q(\text{cm}^3) \times X(\text{cm})}{A(\text{cm}^2) \times t(\text{s}) \times C(\text{cm Hg})} \times \frac{273.15(\text{K})}{T(\text{K})} \times 10^{10}$$

where Q (cm^3) is the volume of the test gas permeated through the membrane, X (cm) is the thickness of the sample membrane, A (cm^2) is the permeation area, t (s) is the sampling time, C (cm Hg) is the partial pressure of the test gas and T (K) is the absolute temperature.

Single-gas permeation tests were performed by introducing a pure tested gas, whereas mixed-gas permeation tests were performed by introducing CO_2/N_2 (2/1 by volume) mixed gases.

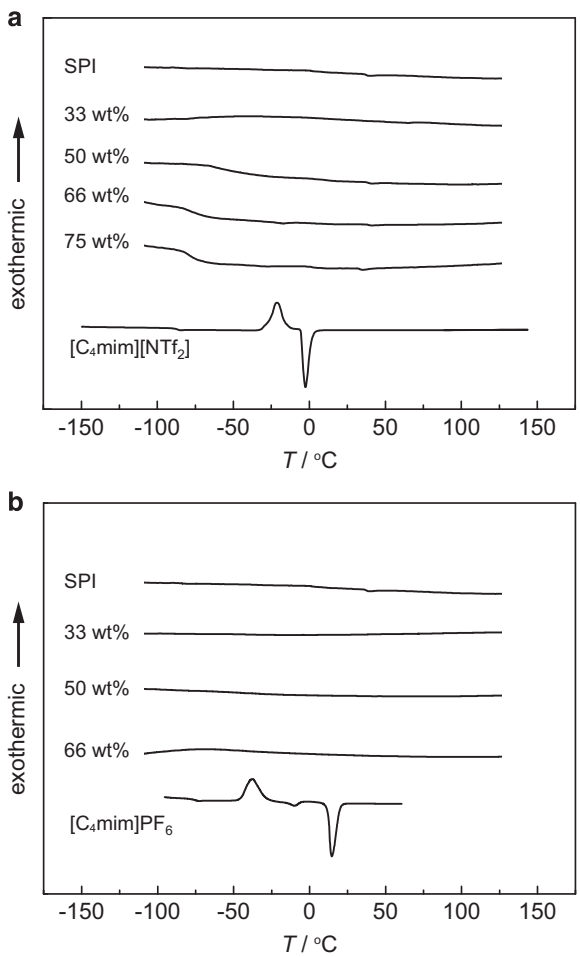

Figure 2 Differential scanning calorimetry (DSC) curves of the pure sulfonated polyimide (SPI) membrane and composite membranes: (**a**) SPI-NTf_2 and (**b**) SPI-PF_6.

RESULTS AND DISCUSSION

Membrane fabrication

In this paper, the IL/SPI composite membranes are denoted as SPI-A (X), where A is the anionic structure of the ILs and X is weight percent (wt%) of the ILs in the composite membranes. For example, SPI-NTf_2 (50) means [C_4mim][NTf_2]/SPI composite membrane including 50 wt % of [C_4mim][NTf_2]. Figure 1c shows the appearance of a composite membrane. For all the compositions except for SPI-PF_6 (75), transparent, flexible and uniform membranes were obtained. Previously, based on the results of atomic force microscopy tapping images, we reported nanophase separation of the ionic soft domain from the non-ionic hard domain in the IL/SPI composite membranes; we also reported that the ILs appeared to be preferentially incorporated into the ionic domain.[45] [C_4mim]PF_6 had lower compatibility with the SPI in comparison with [C_4mim][NTf_2], and thus macroscopic phase separation occurred at higher IL contents. However, when the SPI and the ILs were compatible, homogeneous membranes having thicknesses of 20–150 μm with no leakage of the ILs were obtained. In this study, these membranes were examined using thermal analysis, tensile tests and gas permeation tests.

Differential scanning calorimetry

Figures 2a and b show the DSC curves of the pure ILs, the pure SPI and the composite membranes. [C_4mim][NTf_2] exhibited phase transitions at −87, −22 and −3.1 °C, which can be assigned to the glass transition, crystallization and melting temperatures, respectively, whereas [C_4mim]PF_6 exhibited those transitions at −73, −38, −10 and 15 °C, respectively. These values are comparable to those reported in previous studies.[49–51] On the other hand, no phase transition except for a slight baseline shift, assignable to the glass transition, was observed for each composite membrane at temperatures below −50 °C. The ILs appear to be confined into the nanosize ionic domains, and thus crystallization of the ILs is inhibited (confinement effect).[47]

TG curves of the ILs, SPI and the composite membranes are shown in Figure 3, and the decomposition temperatures are listed in Table 1. The SPI weight loss was observed at 333 °C, whereas those of [C_4mim][NTf_2] and [C_4mim]PF_6 were observed at 413 and 358 °C, respectively. For the composite membranes, the residual weight at the upper limit of the measurement (at 550 °C) changed as a function of the weight ratio of the SPI to the IL. However, the composite membranes did not clearly show two-step weight loss because of the close decomposition temperatures between the SPI and the ILs. It is clear that the composite membranes have sufficient thermal stability for CO_2 gas separation.

Tensile tests

Strain–stress curves measured for the SPI and the composite membranes are shown in Figure 4, and the parameters of the mechanical properties are listed in Table 1. The stress at break, elongation at break and Young's modulus measured for the SPI membrane were 58.7 MPa, 24.1% and 1.58 GPa, respectively. With the addition of the ILs, the yield behavior of the SPI gradually disappeared. These phenomena clearly demonstrate that the ILs functioned as plasticizers in the composite membranes. However, even for SPI-NTf_2

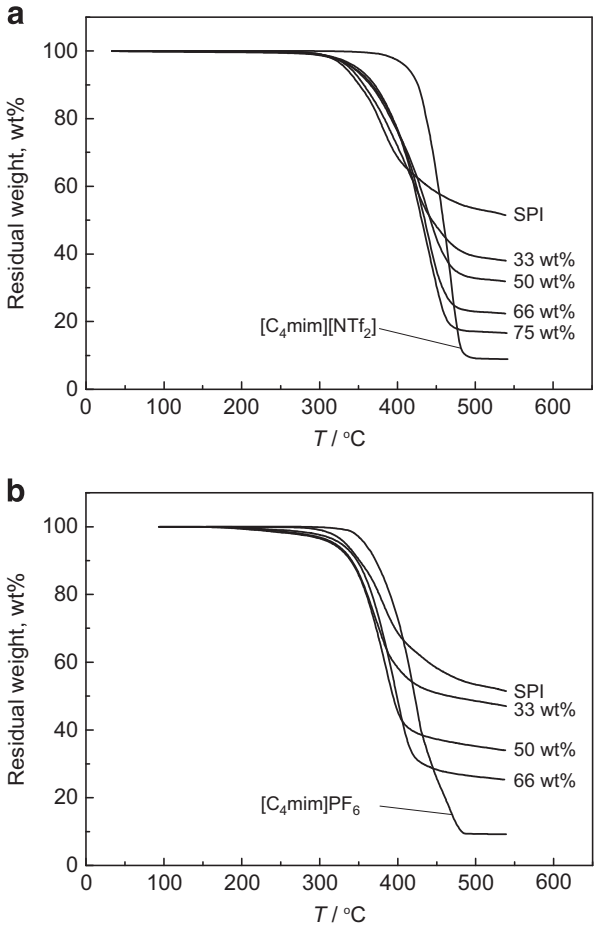

Figure 3 Thermogravimetric (TG) curves of the pure sulfonated polyimide (SPI) membrane and the composite membranes: (**a**) SPI-NTf_2 and (**b**) SPI-PF_6.

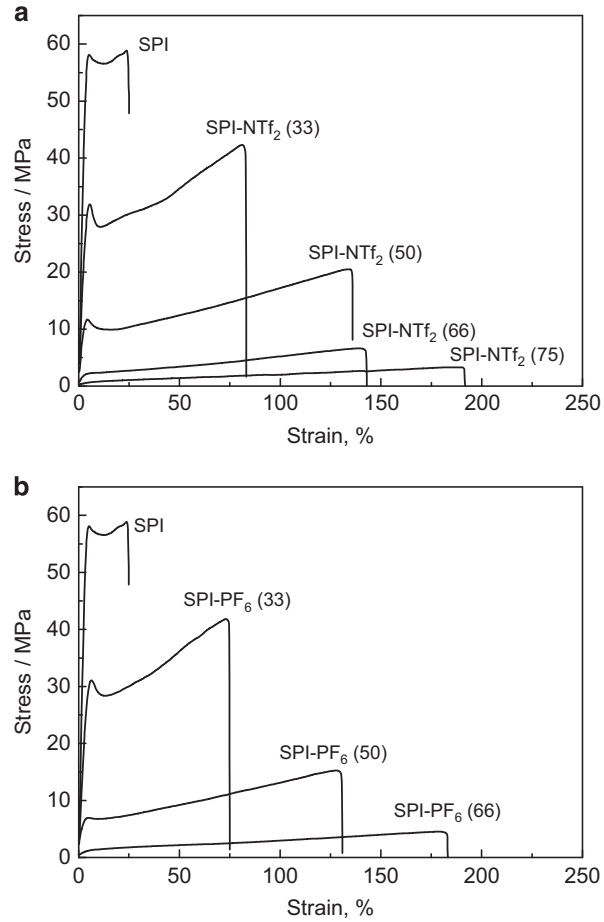

Figure 4 Strain–stress curves of the sulfonated polyimide (SPI) and the composite membranes: (**a**) SPI-NTf_2 and (**b**) SPI-PF_6.

Table 1 The results of TGA and tensile tests

Membranes	*Decomposition[a] temp. (°C)*	*Stress at break (MPa)*	*Strain at break (%)*	*Young's modulus (MPa)*
SPI	333	59	24	1.58×10^3
SPI-NTf_2 (33)	339	42	82	782
SPI-NTf_2 (50)	343	20	135	330
SPI-NTf_2 (66)	348	6.4	142	50.5
SPI-NTf_2 (75)	344	3.2	191	9.55
SPI-PF_6 (33)	319	42	74	637
SPI-PF_6 (50)	316	15	130	135
SPI-PF_6 (66)	327	4.2	182	20.2

Abbreviations: SPI, sulfonated polyimide; TGA, thermogravimetric analysis.
[a]Decomposition temperature is defined as the temperature at 5 wt% weight loss.

(75), the stress at break and Young's modulus were 3.16 and 9.6 MPa, respectively, values that are much greater than those reported for conventional ion gels: It was reported that poly(methyl methacrylate)/TEOS-based composite membrane including 76 wt% of [C_4mim][NTf_2] exhibits ca. 0.3 MPa of Young's modulus,[52] while polyether-based composite membrane exhibits 0.58 MPa.[53] These superior mechanical properties of the IL/SPI composite membranes are preferable for practical applications. Differences in the mechanical behavior of the SPI-NTf_2 and SPI-PF_6 composite membranes were observed but were not significant.

Table 2 The results of gas permeability measurements performed under single- and mixed-gas conditions

Membranes	*Single-gas conditions* $P_{CO_2}/P_{N_2}/\alpha$	*Mixed-gas conditions* $P_{CO_2}/P_{N_2}/\alpha$
SPI	0.58/–/–	–/–/–
SPI-NTf_2 (33)	6.95/0.26/27	5.53/0.35/16
SPI-NTf_2 (50)	35.9/1.24/29	32.2/2.15/15
SPI-NTf_2 (66)	212/7.88/27	136/10.1/13
SPI-NTf_2 (75)	412/15.4/27	378/30.8/12
SPI-PF_6 (33)	4.72/0.15/33	—
SPI-PF_6 (50)	18.8/0.54/35	—
SPI-PF_6 (66)	65.8/1.77/37	—

Abbreviation: SPI, sulfonated polyimide.

Gas permeability

CO_2 and N_2 permeation properties measured under single-gas conditions are listed in Table 2. At 30 °C, the CO_2 permeability of the SPI membrane was 0.58 Barrer. On the other hand, the N_2 permeability could not be measured correctly because the N_2 gas permeation of the membrane was too low to be detected by our instrument. This result indicates that the SPI membranes have low gas permeability, comparable to those of typical polyimide membranes[54,55] (e.g., Kapton), which have high T_g and very low gas

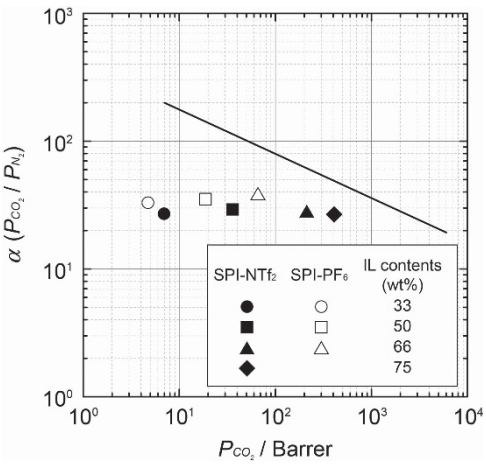

Figure 5 Robeson plot of sulfonated polyimide/ionic liquid (SPI/IL) composite membrane. Solid line indicates upper limit for CO_2 separation polymer membranes reported in Robeson.[56]

permeability. This suggests that the substitution of sulfonic acid groups into a polyimide structure does not greatly affect the gas barrier properties. The much higher CO_2 permeability than N_2 permeability through the SPI membrane can be explained by the higher solubility of CO_2 into the SPI membrane due to the stronger interaction of CO_2 with the SPI by a quadrupole moment than non-polar N_2. It should be noted that the gas permeability greatly increased by the addition of the IL and that the P_{CO_2} and P_{N_2} values of SPI-NTf$_2$ (75) at 30 °C reached 412 Barrer and 15.4 Barrer, respectively, whereas those of SPI-PF$_6$ (66) were 65.8 Barrer and 1.77 Barrer, respectively. Interestingly, the separation coefficient ($\alpha = P_{CO_2}/P_{N_2}$) seems to depend on the IL structures. The α-values of SPI-NTf$_2$ and SPI-PF$_6$ were 27–29 and 33–37, respectively. No significant decrease in α was observed, even with the increase in gas permeability, accompanied by increasing IL content. These results suggest that the permeability of the gases is mainly dominated by the solubility of the gases in the membranes, where the ionic groups form domains, that the ILs are preferentially incorporated into the ionic domains and that both gases selectively permeate in the ionic domain.

The gas permeation properties under mixed-gas conditions were also investigated for the SPI-NTf$_2$ composite membrane, and the results are listed in Table 2. As compared with the gas permeability under single-gas conditions, P_{CO_2} decreased, whereas P_{N_2} increased. This phenomenon has been often reported for mixed-gas measurements. Two explanations are generally accepted. One is based on plasticization effect of CO_2 molecule for matrix membrane. If membrane is plasticized by CO_2 molecule, free volume in the membrane increases and thus gas permeation coefficient increases. Therefore, CO_2 permeation coefficient may decrease with decreasing partial pressure of CO_2 in test gas. Simultaneously, in the case of CO_2/N_2 mixture, N_2 permeation coefficient will increase with decreasing partial pressure of N_2, since partial pressure of CO_2 increases. The other explanation is based on dragging effect. When two gases having different diffusion coefficients are used for mixed-gas measurements, faster diffusing gas molecule is dragged by slower diffusing one and becomes slower. In contrast, slower diffusing gas is dragged by faster diffusing one and becomes faster. As a result, the separation coefficient decreases. Actually, both mechanisms may cause the same result. To conclude which mechanism is plausible for IL/SPI composite membrane, further investigation is required. Finally, the separation performance of our composite membranes is demonstrated in Robson plots, shown in Figure 5, where the upper limits of the gas permeation polymer membranes are shown with solid lines.[56] The results are still below the upper limit; however, they approach the limit with increasing IL content.

CONCLUSION

A series of composite membranes, SPI-NTf$_2$ and SPI-PF$_6$, were prepared and their thermal, mechanical and gas permeation properties were investigated. SPI showed good compatibility with ILs and thus ILs functioned as plasticizer of SPI. However, SPI composite membrane exhibited much high Young's modulus (≈10 MPa) even when it includes 75 wt% of ILs. This characteristic is convenient for fabricate thin membrane. The SPI membrane behaved as a gas barrier membrane (P_{CO_2} for SPI membrane is 0.58 Barrer). However, the addition of ILs greatly enhanced the gas permeability to be 412 Barrer for SPI-NTf$_2$ (75). The SPI-PF$_6$ composite membranes slightly lower the gas permeability than SPI-NTf$_2$ composite membranes at same IL contents, but higher separation coefficient ($\alpha = P_{CO_2}/P_{N_2}$). In the permeation tests under mixed-gas conditions, P_{CO_2} and P_{N_2} values were lower and higher, respectively, than those under single-gas conditions. However, α-value was maintained in the range 12–16.

CONFLICT OF INTEREST

The authors declare no conflict of interest.

ACKNOWLEDGEMENTS

This work was financially supported by the Grant-in-Aid for Scientific Research S (15H05495) from Ministry of Education, Culture, Sports, Science and Technology (MEXT) of Japan.

1 Chow, J. C., Watson, J. G., Herzog, A., Benson, S. M., Hidy, G. M., Gunter, W. D., Penkala, S. J. & White, C. M. Separation and capture of CO_2 from large stationary sources and sequestration in geological formations. *J. Air Waste Manage. Assoc.* **53**, 1172–1182 (2003).
2 Karadas, F., Atilhan, M. & Aparicio, S. Review on the use of ionic liquids (ILs) as alternative fluids for CO_2 capture and natural gas sweetening. *Energy Fuels* **24**, 5817–5828 (2010).
3 Myers, C., Pennline, H., Luebke, D., Ilconich, J., Dixon, J. K., Maginn, E. J. & Brennecke, J. F. High temperature separation of carbon dioxide/hydrogen mixtures using facilitated supported ionic liquid membranes. *J. Membr. Sci.* **322**, 28–31 (2008).
4 Zeng, S., Wang, J., Bai, L., Wang, B., Gao, H., Shang, D., Zhang, X. & Zhang, S. Highly selective capture of CO_2 by ether-functionalized pyridinium ionic liquids with low viscosity. *Energy Fuels* **29**, 6039–6048 (2015).
5 Huang, K., Zhang, X.-M., Xu, Y., Wu, Y.-T. & Hu, X.-B. Protic ionic liquids for the selective absorption of H_2S from CO_2: thermodynamic analysis. *AIChE J.* **60**, 4232–4240 (2014).
6 Yang, H., Xu, Z., Fan, M., Gupta, R., Slimane, R. B., Bland, A. E. & Wright, I. Progress in carbon dioxide separation and capture: a review. *J. Environ. Sci.* **20**, 14–27 (2008).
7 Freeman, S. A., Dugas, R., Wagener, D. V., Nguyen, T. & Rochelle, G. T. Carbon dioxide capture with concentrated, aqueous piperazine. *Energy Proc.* **1**, 1489–1496 (2009).
8 Lei, Z., Dai, C. & Chen, B. Gas solubility in ionic liquids. *Chem. Rev.* **114**, 1289–1326 (2014).
9 To, J. W. F., He, J., Mei, J., Haghpanah, R., Chen, Z., Kurosawa, T., Chen, S., Bae, W.-G., Pan, L., Tok, J B-H, Wilcox, J. & Bao, Z. Hierarchical n-doped carbon as CO_2 adsorbent with high CO_2 selectivity from rationally designed polypyrrole precursor. *J. Am. Chem. Soc.* **138**, 1001–1009 (2016).
10 Liu, Y., Wang, Z. U. & Zhou, H.-C. Recent advances in carbon dioxide capture with metal-organic frameworks. *Greenhouse Gas Sci. Technol.* **2**, 239–259 (2012).
11 Kenarsari, S. D., Yang, D., Jiang, G., Zhang, S., Wang, J., Russell, A. G., Wei, Q. & Fan, M. Review of recent advances in carbon dioxide separation and capture. *RSC Adv.* **3**, 22739–22773 (2013).
12 Baker, R. W. & Lokhandwala, K. Natural gas processing with membranes: an overview. *Ind. Eng. Chem. Res.* **47**, 2109–2121 (2008).
13 Koros, W. J. & Fleming, G. K. Membrane-based gas separation. *J. Membr. Sci.* **83**, l–80 (1993).
14 Scovazzo, P., Kieft, J., Finan, D. A., Koval, C., DuBois, D. & Noble, R. Gas separations using non-hexafluorophosphate $[PF_6]^-$ anion supported ionic liquid membranes. *J. Membr. Sci.* **238**, 57–63 (2004).

15 Baltus, R. E., Counce, R. M., Culbertson, B. H., Luo, H., DePaoli, D. W., Dai, S. & Duckworth, D. C. Examination of the potential of ionic liquids for gas separations. *Sep. Sci. Technol.* **40**, 525–541 (2005).
16 Hanioka, S., Maruyama, T., Sotani, T., Teramoto, M., Matsuyama, H., Nakashima, K., Hanaki, M., Kubota, F. & Goto, M. CO_2 separation facilitated by task-specific ionic liquids using a supported liquid membrane. *J. Membr. Sci.* **314**, 1–4 (2008).
17 Bara, J. E., Carlisle, T. K., Gabriel, C. J., Camper, D., Finotello, A., Gin, D. L. & Noble, R. D. Guide to CO_2 separations in imidazolium-based room-temperature ionic liquids. *Ind. Eng. Chem. Res.* **48**, 2739–2751 (2009).
18 Powell, C. E. & Qiao, G. G. Polymeric CO_2/N_2 gas separation membranes for the capture of carbon dioxide from power plant flue gases. *J. Membr. Sci.* **279**, 1–49 (2006).
19 Tomé, L. C., Mecerreyes, D., Freire, C. S. R., Rebelo, L. P. N. & Marrucho, I. M. Pyrrolidinium-based polymeric ionic liquid materials: new perspectives for CO_2 separation membranes. *J. Membr. Sci.* **428**, 260–266 (2013).
20 Bara, J. E., Camper, D. E., Gin, D. L. & Noble, R. D. Room-temperature ionic liquids and composite materials: platform technologies for CO_2 capture. *Acc. Chem. Res.* **43**, 152–159 (2010).
21 Bara, J. E., Noble, R. D. & Gin, D. L. Effect of 'free' cation substituent on gas separation performance of polymer-room-temperature ionic liquid composite membranes. *Ind. Eng. Chem. Res.* **48**, 4607–4610 (2009).
22 Bara, J. E., Hatakeyama, E. S., Gin, D. L. & Noble, R. D. Improving CO_2 permeability in polymerized room-temperature ionic liquid gas separation membranes through the formation of a solid composite with a room-temperature ionic liquid. *Polym. Adv. Techno.l* **19**, 1415–1420 (2008).
23 Hong, S. U., Park, D., Koa, Y. & Baek, I. Polymer-ionic liquid gels for enhanced gas transport. *Chem. Commun.* **46**, 7227–7229 (2009).
24 Jansen, J. C., Friess, K., Clarizia, G., Schauer, J. & Izák, P. High ionic liquid content polymeric gel membranes: preparation and performance. *Macromolecules* **44**39–45 (2011).
25 Gu, Y. & Lodge, T. P. Synthesis and gas separation performance of triblock copolymer ion gels with a polymerized ionic liquid mid-block. *Macromolecules* **44**, 1732–1736 (2011).
26 Li, P., Pramoda, K. P. & Chung, T.-S. CO_2 separation from flue gas using polyvinyl-(room temperature ionic liquid)-room temperature ionic liquid composite membranes. *Ind. Eng. Chem. Res.* **50**, 9344–9353 (2011).
27 Fujii, K., Makino, T., Hashimoto, K., Sakai, T., Kanakubo, M. & Shibayama, M. Carbon dioxide separation using a high-toughness ion gel with a tetra-armed polymer network. *Chem. Lett.* **44**, 17–19 (2015).
28 Blanchard, L. A., Hancu, D., Beckman, E. J. & Brennecke, J. F. Green processing using ionic liquids and CO_2. *Nature* **399**, 28–29 (1999).
29 Hoffmann, M. M., Heitz, M. P., Carr, J. B. & Tubbs, J. D. Surfactants in green solvent systems—current and future research directions. *J. Dispers. Sci. Technol.* **24**, 155–171 (2003).
30 Huddleston, J. G., Visser, A. E., Reichert, W. M., Willauer, H. D., Broker, G. A. & Rogers, R. D. Characterization and comparison of hydrophilic and hydrophobic room temperature ionic liquids incorporating the imidazolium cation. *Green Chem.* **3**, 156–164 (2001).
31 Welton, T. Room-temperature ionic liquids. solvents for synthesis and catalysis. *Chem. Rev.* **99**, 2071–2083 (1999).
32 Lodge, T. P. A unique platform for materials design. *Science* **321**, 50–51 (2008).
33 Susan, M. A. B. H., Kaneko, T., Noda, A. & Watanabe, M. Ion gels prepared by in situ radical polymerization of vinyl monomers in an ionic liquid and their characterization as polymer electrolytes. *J. Am. Chem. Soc.* **127**, 4976–4983 (2005).
34 He, Y., Boswell, P. G., Bu1hlmann, P. & Lodge, T. P. Ion gels by self-assembly of a triblock copolymer in an ionic liquid. *J. Phys. Chem. B* **111**, 4645–4652 (2007).
35 He, Y. & Lodge, T. P. A thermoreversible ion gel by triblock copolymer self-assembly in an ionic liquid. *Chem. Commun.* **26**, 2732–2734 (2007).
36 He, Y. & Lodge, T. P. Thermoreversible ion gels with tunable melting temperatures from triblock and pentablock copolymers. *Macromolecules* **41**, 167–174 (2008).
37 Kitazawa, Y., Ueki, T., Niitsuma, K., Imaizumi, S., Lodge, T. P. & Watanabe, M. Thermoreversible high-temperature gelation of an ionic liquid with poly(benzyl methacrylate-*b*-methyl methacrylate-*b*-benzyl methacrylate) triblock copolymer. *Soft Matter.* **8**, 8067–8074 (2012).
38 Ueki, T., Nakamura, Y., Usui, R., Kitazawa, Y., So, S., Lodge, T. P. & Watanabe, M. Photoreversible gelation of a triblock copolymer in an ionic liquid. *Angew. Chem. Int. Ed.* **54**, 3018–3022 (2015).
39 Ma, X., Usui, R., Kitazawa, Y., Kokubo, H. & Watanabe, M. Photo-healable ion gel with improved mechanical properties using a tetra-arm diblock copolymer containing azobenzene groupsPolymer **78**, 42–50 (2015).
40 Ma, X., Usui, R., Kitazawa, Y., Kokubo, H. & Watanabe, M. Temperature and light-induced self-assembly changes of a tetra-arm diblock copolymer in an ionic liquid. *Polym. J.* **47**, 739–746 (2015).
41 Noro, A., Matsushita, Y. & Lodge, T. P. Thermoreversible supramacromolecular ion gels via hydrogen bonding. *Macromolecules* **41**, 5839–5844 (2008).
42 Noro, A., Matsushita, Y. & Lodge, T. P. Gelation mechanism of thermoreversible supramacromolecular ion gels via hydrogen bonding. *Macromolecules* **42**, 5802–5810 (2009).
43 Bernardo, P., Drioli, E. & Golemme, G. Membrane gas separation: a review/state of the art. *Ind. Eng. Chem. Res.* **48**, 4638–4663 (2009).
44 Lee, S.-Y., Yasuda, T. & Watanabe, M. Fabrication of protic ionic liquid/sulfonated polyimide composite membranes for non-humidified fuel cells. *J. Power Sources* **195**, 5909–5914 (2010).
45 Yasuda, T., Nakamura, S., Honda, Y., Kinugawa, K., Lee, S.-Y. & Watanabe, M. Effects of polymer structure on properties of sulfonated polyimide/protic ionic liquid composite membranes for nonhumidified fuel cell applications. *ACS Appl. Mater. Interfaces* **4**, 1783–1790 (2012).
46 Lee, S.-Y., Ogawa, A., Kanno, M., Nakamoto, H., Yasuda, T. & Watanabe, M. Nonhumidified intermediate temperature fuel cells using protic ionic liquids. *J. Am. Chem. Soc.* **132**, 9764–9773 (2010).
47 Yasuda, T. & Watanabe, M. Protic ionic liquids: fuel cell applications. *MRS Bull.* **38**, 560–566 (2013).
48 Imaizumi, S., Ohtsuki, Y., Yasuda, T., Kokubo, H. & Watanabe, M. Printable polymer actuators from ionic liquid, soluble polyimide, and ubiquitous carbon materials. *ACS Appl. Mater. Interfaces* **5**, 6307–6315 (2013).
49 Tokuda, H., Ishii, K., MABH, Susan, Tsuzuki, S., Hayamizu, K. & Watanabe, M. Physicochemical properties and structures of room-temperature ionic liquids. 3. Variation of cationic structures. *J. Phys. Chem. B* **110**, 2833–2839 (2006).
50 Strehmel, V., Rexhausen, H., Strauch, P. & Strehmel, B. Temperature dependence of interactions between stable piperidine-1-yloxyl derivatives and a semicrystalline ionic liquid. *ChemPhysChem* **11**, 2182–2190 (2010).
51 Endo, T., Kato, T., Tozaki, K. & Nishikawa, K. Phase behaviors of room temperature ionic liquid linked with cation conformational changes: 1-butyl-3-methylimidazolium hexafluorophosphate. *J. Phys. Chem. B* **114**, 407–411 (2010).
52 Gayet, F., Viau, L., Leroux, F., Monge, S., Robin, J.-J. & Vioux, A. Polymer nanocomposite ionogels, high-performance electrolyte membranes. *J. Mater. Chem.* **20**, 9456–9462 (2010).
53 Matsumoto, K. & Endo, T. Synthesis of ion conductive networked polymers based on an ionic liquid epoxide having a quaternary ammonium salt structure. *Macromolecules* **42**, 4580–4584 (2009).
54 Liaw, D.-J., Wang, K.-L., Huang, Y.-C., Lee, K.-R., Lai, J.-Y. & Ha, C.-S. Advanced polyimide materials: syntheses, physical properties and applications. *Prog. Polym. Sci.* **37**, 907–974 (2012).
55 Xiao, Y., Low, B. T., Hosseini, S. S., Chung, T. S. & Paul, D. R. The strategies of molecular architecture and modification of polyimide-based membranes for CO_2 removal from natural gas—a review. *Prog. Polym. Sci.* **34**, 561–580 (2009).
56 Robeson, L. M. The upper bound revisited. *J. Membr. Sci.* **320**, 390–400 (2008).